Limnol. Oceanogr., 59(4), 2014, 1181–1192

doi:10.4319/lo.2014.59.4.1181

Application of stable isotope mixing models for defining trophic biomagnification pathways of mercury and selenium

H. J. Jones,[1,*] K. M. Swadling,[1] E. C. V. Butler,[2] L. A. Barry,[3] and C. K. Macleod [1]

[1] Institute for Marine and Antarctic Studies, University of Tasmania, Hobart, Tasmania, Australia
[2] Australian Institute of Marine Science, Casuarina, Northern Territory, Australia
[3] Australian Nuclear Science and Technology Organisation, Lucas Heights, New South Wales, Australia

Abstract

Trophic models based on nitrogen stable isotope ratios ($\delta^{15}N$) have been shown to predict changes in mercury (Hg) concentrations in fish; however, they are usually applied at the ecosystem scale and are rarely directed at known trophic pathways. We discuss a novel approach in which we combined gut contents analysis and stable isotope analyses ($\delta^{15}N$ and $\delta^{13}C$) into a Bayesian isotopic mixing model to provide a quantitative estimate of Hg and selenium (Se) biomagnification in an estuarine food web. Estimates of the relationship between total mercury (THg) and methylmercury (MeHg) were significantly improved in mixing model-adjusted food webs over models that included all known prey sources. Spatial differences in dietary composition and MeHg bioavailability offer strong evidence that local food webs can have a significant effect on the biomagnification of Hg within benthic fish species. While no evidence of Se biomagnification was found, lower Se : Hg ratios at higher trophic levels could be attributed to increasing trophic Hg concentration. Furthermore, stable isotope analysis suggested Hg and Se biotransfer from benthic sources to fish. Overall, the findings highlight that isotope mixing models can be a significant aid in assessments of contaminant biomagnification, particularly when it is important to define food pathways to top predators.

To delineate the pathways involved in the accumulation of mercury (Hg) and selenium (Se) in marine organisms, it is necessary to examine the trophic position of the species and the route of biomass acquisition (Wang 2002; Chen et al. 2009). Total mercury (THg) and methylmercury (MeHg) concentrations typically increase with trophic level (Beneditto et al. 2012), as can Se concentrations (Besser et al. 1993; Wang 2002; Hamilton 2004). The role of Se in mitigating Hg toxicity (Yang et al. 2008; Kehrig et al. 2009; Peterson et al. 2009) has led to recent work quantifying Hg and Se concentration against trophic position (Campbell et al. 2005; Hong et al. 2013; Karimi et al. 2013). Consumers' tissues are ultimately derived from the food they eat; consequently, stable isotope ratios of carbon ($\delta^{13}C$) and $\delta^{13}C$ nitrogen ($\delta^{15}N$) offer an effective quantitative measure of trophic structure, providing time-integrated tracers of energy flow, dietary history, and trophic position (Post 2002; Phillips and Gregg 2003). Carbon (C) isotope ratios ($\delta^{13}C$) provide a biomarker of organic C production, enabling identification of primary production and bioaccumulated contaminant sources (France 1995; Chen et al. 2009; Gehrke et al. 2011). Nitrogen isotope ratios ($\delta^{15}N$) exhibit a constant rate of incremental enrichment between trophic levels (typically 3.4‰), supplying a quantitative measure of trophic hierarchy (Post 2002) against which contaminant biomagnification can be assessed (Cheung and Wang 2008; Tom et al. 2010). Regression slopes between $\log_{10}$Hg and $\delta^{15}N$ are used as a measure of Hg biomagnification in ecosystems (Chen et al. 2009; Coelho et al. 2013). Notably, $\log_{10}$Hg–$\delta^{15}N$ regression slopes appear relatively constant (~ 0.2) despite changes in aquatic habitats, Hg source, and food pathways (Campbell et al. 2005; Al-Reasi et al. 2007; Chen et al. 2009). Biomagnification studies based on stable isotope ratios alone are limited, as they cannot differentiate the importance of different prey sources with similar isotopic signatures. Although food web studies based on dietary content can distinguish between prey source contributions, they represent only a snapshot of food availability and provide no evidence of long-term diet (Chen et al. 2009; Cossa et al. 2012).

Bayesian stable isotope mixing models (BSIMM) have been designed specifically to allow incorporation of prior information (stomach contents), to account for multiple prey sources, and to estimate the proportional contribution of prey to consumer tissues (Phillips and Gregg 2003; Moore and Semmens 2008). Not all prey consumed by a predator contribute significantly to predatory biomass despite sharing similar $\delta^{13}C$ values, and BSIMM can quantify source contributions, in turn allowing elimination of nonsignificant sources (Bond and Diamond 2011). Contaminant–$\delta^{15}N$ regressions optimized by preliminary BSIMM may offer a solution to identifying key species responsible for the transport of contaminants and may assist in refining model fit.

Intraestuarine variation in feeding strategies and available prey have been shown to result in major changes in both stable isotope signatures and Hg concentration of estuarine fish (Adams and Paperno 2012). In the Derwent Estuary, Tasmania, both Se and Hg contamination occur in a predatory fish species, sand flathead (*Platycephalus bassensis*) (Jones et al. 2013*a*), as a result of point-source industry inputs (Dix et al. 1975; Bloom and Ayling 1977). Small-scale spatial variation in contaminant concentrations for this species may be a result of dietary-related biomagnification differences (Jones et al. 2013*a,b*). The

* Corresponding author: hjones1@utas.edu.au

aims of this study were to (1) quantify the trophic position of sand flathead and its prey through stable isotope analysis and determine key food pathways through gut contents and BSIMM; (2) compare and contrast spatial variability in the trophic magnification of THg, MeHg, and Se; and (3) evaluate the effectiveness of applying BSIMM to the patterns of trophic biomagnification in this particular food pathway.

Method

Study region—The Derwent Estuary, located in southern Tasmania (42°53′44 S, 147°22′08 E; Fig. 1), is a microtidal (1.2 m) estuary, 52 km in length and with a maximum depth of 30 m (Green and Coughanowr 2003). The choice of study regions was based on previous research assessing THg, MeHg, and Se concentration in sand flathead (Jones et al. 2013*a,b*) and sediments (Jones et al. 2014). Two estuary regions were selected: the industrialized Middle Estuary (ME), which has consistently high THg concentrations in sediments and flathead, and Ralphs Bay (RB), a large and relatively shallow embayment on the lower eastern side of the estuary that exhibits relatively low THg levels in the sediment (Jones et al. 2003, 2014) but high THg concentrations in fish (Jones et al. 2013*b*). A reference region, Mickey's Bay (MB), located south of the estuary, was included to provide comparative concentrations from a region that has not been contaminated with heavy metals (Jones et al. 2013*b*, 2014; Fig. 1).

Sample collection—All containers and apparatus used in sample processing were either high-density polyethylene (HDPE) or, where available, polytetrafluoroethylene (Teflon). Acid-cleaned (10–20% HCL, 1 week bath) laboratory and noncontaminating techniques were employed throughout all sample processing and storage steps.

Fish: Sixty fish were sampled in November–December 2011 by line fishing. Fish were individually sealed in plastic bags, stored on ice, and frozen (−40°C). Processing followed the procedure described by Verdouw et al. (2011): morphometric measurements of each fish included fork length (± 1 mm), wet weight (whole ± 0.1 g), and sex. The stomach of each fish was weighed full, and the contents were then separated into lowest determinable taxonomic groups. These groups were weighed, and the number of individuals was counted. Whole fish, minus stomach contents, were lyophilized to constant mass (± 0.1 g) and homogenized.

Invertebrate prey: Two sampling methods were used for the collection of invertebrates: a dredge (mesh size: 2 mm sides, 12 mm base) towed behind a vessel for approximately 100 m and a venturi pump (aperture: 90 mm) operated by divers. In both cases, once the samples were retrieved, the collected material was washed thoroughly in mesh bags (1 mm mesh) before being placed on ice. Samples were sorted immediately on return to the laboratory. Representatives of species that had previously been observed in the stomach contents of sand flathead were isolated from the bulk samples and left to purge overnight in aerated, filtered seawater (0.4 μm). Composite samples were prepared for each of these species, where individuals with weight or size similar to those in the gut samples were selected and pooled. These samples were then lyophilized, homogenized, and subsplit for THg, MeHg, Se, δ^{13}C, and δ^{15}N analyses.

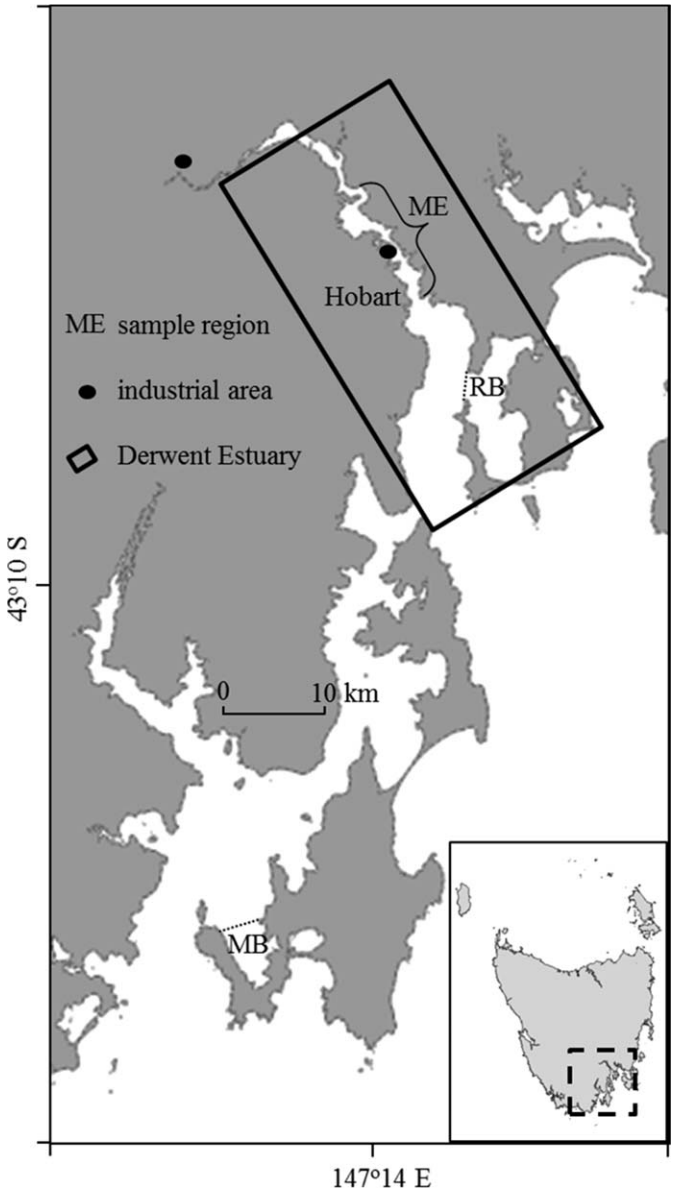

Fig. 1. Southern Tasmania and location of the Derwent Estuary (boxed), with locations of the two estuary regions, ME and RB, and location of reference region (MB) 48 km south.

Prey fish: Undigested individual fish were extracted from the gut contents of sand flathead and thoroughly washed in reverse-osmosis (RO) water (Elga Purelab Prima) to remove contaminants. Positive identification of species was generally prohibited by the initial stages of digestion; however, provided that the majority of the fish was present (i.e., muscle, vertebrae, head), they were lyophilized, homogenized, and subsplit for THg, MeHg, Se, δ^{13}C, and δ^{15}N analyses.

Plankton: Two size fractions of plankton (63–200 μm and $>$ 200 μm) were collected from a drifting vessel on four occasions at each region between September 2010 and April 2012. Diagonal tows of 63 μm and 200 μm nets were taken

from approximately 1 m above the seabed to the surface. The 63 μm samples were backwashed with filtered seawater (0.4 μm) into HDPE containers fitted with 200 μm mesh to remove the larger fraction. The containers were placed in a positive pressure glove bag where they were aerated overnight to allow the plankton time to purge. After purging, each sample was split into two equal parts, one for THg, MeHg, and Se analyses and the other for stable isotope analysis. Subsamples for trace element (THg, MeHg, and Se) and stable isotope analyses were captured onto 0.4 μm filters in the glove bag and scraped clean. Samples were lyophilized prior to analysis.

Trace element analysis—Digestions and analyses were performed using the method described in Jones et al. (2013*a*).

THg, MeHg, and Se digestion: THg and Se samples were digested for 2 h in HNO_3 (trace grade) in polypropylene digestion vessels at 120°C within a deep cell digestion block. H_2O_2 was added to each sample, and the vessels were digested for a further 1 h before HNO_3 : HCl mixture (3 : 1) was then added to the vessels and heated for 1 h. Samples were diluted to 50 mL total volume with RO water and analyzed within 48 h of digestion. MeHg extraction followed a serial extraction using KOH, then HCl, and finally a solution of $CuSO_4$-KBr-H_2SO_4. Dichloromethane (DCM) was added, and the vials were returned to the shaker overnight. The DCM layer was then transferred to a clean glass vial, and 0.01 mol L^{-1} sodium thiosulphate ($Na_2S_2O_3$; 2 mL) was used to extract the MeHg component. The final extract was filtered (0.45 μm) before analysis.

THg analysis: Analysis was carried out by cold vapor atomic fluorescence spectroscopy (10.023 Millenium Merlin, PS Analytical). A 2% w : v tin(II) chloride reductant and argon (Ar) carrier gas was used.

MeHg analysis: Aliquots were analyzed by high-pressure liquid chromatography–ultraviolet–atomic fluorescence spectroscopy using an oxidant stream of acidified potassium bromide-potassium bromate (10% v : v HCl, 10% v : v 0.1 M Br^-–BrO_3^-). A 38% methanol, 30% acetonitrile (m : v) with ammonium pyrrolidine dithiocarbamate (0.2464 g L^{-1}) solution was used for the mobile phase with a Supelco C18 column (ODS-2) to provide species separation. An online UV photolysis-heater (Peter Stockwell Analytical [PSA] S570U100) and cooling module (PSA S570C100) coupled to the AFS provided oxidation before analysis. A 2% w : v tin(II) chloride reductant and Ar carrier gas were used for cold vapor separation prior to AFS detection.

Se: Se detection used online prereduction of Se with hydride-generated atomic fluorescence analysis (Millenium Excalibur, PS Analytical). Se was reduced by mixing with prereductant KBr-HCl (5% KBr, 50% HCl) and passing through a UV heater (PSA S570U100; 150°C) and cooling module (PSA S570C100). The sample was then mixed with the reductant (0.7% $NaBH_4$ 0.4% NaOH) to form selenium hydride and carried by Ar (0.3 L min^{-1}) to the detection system.

Quality assurance—Linear calibration was acquired using standards diluted in the appropriate concentration range with matrix-matched reagents. The accuracy was verified with an independent substandard for each of the three analytical procedures. Matrix-matched procedural blanks were analyzed at the beginning and end of sample runs to test for any procedural contamination, with none observed. Calibration verification (independent check and certified reference material) was run after instrument calibration, after every 20 samples, and at the end of each batch of samples. Each sample was run in duplicate, with one sample per batch spiked with 5 ng g^{-1} standard solution and recovery rates recorded. Certified reference materials DOLT-4 (National Research Council Canada, dogfish liver; mean recovery [n = 6] THg = 94.40%, Se = 92.67%, MeHg = 98.66%) and BCR 422 (Institute for Reference Materials and Measurements, cod muscle; mean recovery [n = 6] MeHg = 117.44%) were used to verify recovery rates. All results are reported as dry weight (dry wt).

Stable isotope analysis—Samples were analyzed for $\delta^{13}C$ and $\delta^{15}N$ by isotope ratio mass spectrometry (IsoPrime). The $\delta^{13}C$ and $\delta^{15}N$ results are presented as deviations from standards, expressed as $\delta^{13}C$ and $\delta^{15}N$, using the following formula:

$$\delta X = [R_{sample}/R_{standard} - 1] \times 10^3 \quad (1)$$

where X is ^{13}C or ^{15}N and R is ^{13}C : ^{12}C or ^{15}N : ^{14}N. The reference materials used were, for $\delta^{13}C$, an International Atomic Energy Agency (IAEA) reference material, IAEA C8, with an agreed value of ^{13}C Vienna-Pee Dee Belemnite = −18.31‰ and $\delta^{15}N$; two IAEA reference materials, IAEA N-2 (consensus value atmospheric N [δ^{15}NAIR] = +20.3‰) and IAEA N-3 (consensus value δ^{15}NAIR = +4.7‰); and a U.S. Geological Survey reference material, USGS-34 (consensus value δ^{15}NAIR = −1.8‰). Precision of instrument estimates was 0.1‰ for C and 0.2‰ for N. Duplicate samples were run for all samples and further repeats run if standard deviations between duplicates exceeded 0.4‰.

Statistical analysis—All statistical analyses were performed using the R statistical package (version 3.0.0; R Foundation 2012). Percentage frequency of occurrence (%F) and percentage relative weight (%W) of species in sand flathead stomachs were calculated using the formulae published by Hyslop (1980). Kruskal–Wallis nonparametric tests and ANOVA with unplanned post hoc comparison of means (Tukey honestly significant difference test) were used to test for differences in trace element concentrations and stable isotopes between regions. The THg : Se ratios were calculated by conversion of dry-wt concentrations into molar mass in order to assess molar excess:

$$\text{Se : Hg} = \text{concentration in mg kg}^{-1}\text{(dry wt)/molar mass}$$
$$(\text{Hg} = 200.59,\ \text{Se} = 78.96) \quad (2)$$

A Bayesian isotopic mixing model R package, Stable Isotope Analysis in R (SIAR; Parnell et al. 2010), was used to assess contribution of prey items to diet within each region. The model uses $\delta^{13}C$ and $\delta^{15}N$ data via Markov

Table 1. Stomach contents of *Platycephalus bassensis* (n = 40 per region) sampled from three regions in southern Tasmania, two Derwent regions (ME and RB) and MB. $\%F$ = frequency of occurrence percentage: the number of stomachs containing a given prey item divided by the total number of nonempty stomachs multiplied by 100. $\%W$ = relative weight percentage: the total weight of a given prey item divided by the total weight of all prey items in all stomachs multiplied by 100. BSIMM mean proportional contribution (%) to diet calculated from $\%W$, δ^{15}N, and δ^{13}C of prey and consumer (Parnell et al. 2010).

	$\%F$			$\%W$			BSIMM		
Species	ME	RB	MB	ME	RB	MB	ME	RB	MB
Paragrapsus gaimardii	59.5	82.6	2.5	62.0	40.4	16.9	76.0	57.3	20.4
Petrolisthes elongatus	5.0	12.5	1.0	2.5	10.5	0.9	2.7	16.1	1.1
Halicarcinus ovatus	5.0	2.5	7.5	0.3	1.0	4.7	1.3	2.4	5.4
Macrophthalmus latifrons	27.5	5.0	0	11.6	3.7	0	16.9	5.3	—
Munida haswelli	—	1.0	25.0	—	—	24.1	—	—	29.3
Palaemon intermedius	2.5	2.5	2.5	0.3	1.0	3.7	1.0	1.9	6.4
Caprella sp.	—	2.5	—	—	0	—	—	—	—
Teleost spp.	3.2	5.0	7.5	1.2	10.1	20.0	2.1	17.0	37.4
Unidentifiable	0	2.5	5.0	2.7	23.1	29.7	—	—	—

chain Monte Carlo permutations to produce simulations of dietary proportions of sources to a mixture (predator). SIAR allows incorporation of prior information to drive the model and reduce uncertainty (Parnell et al. 2010). In this study, $\%W$ of diet was used to guide the SIAR model for dietary contributions, with the unidentified $\%W$ proportion split equally between identified prey. Trophic enrichment factors (TEF) were based on mean trophic fractionations with large standard deviations that are considered global averages (TEF $\delta^{13}C = 0.4 \pm 1.3$; TEF $\delta^{15}N = 3.4 \pm 1$) (Post 2002), as no published values were available for the species sampled.

Trophic level (TL) was established through δ^{15}N ratios:

$$TL = [(\delta^{15}N_{species} - \delta^{15}N_{base})/\delta^{15}N] + TL_{base} \quad (3)$$

where $\delta^{15}N_{species}$ is the δ^{15}N value of the species in question, $\delta^{15}N_{base}$ is the δ^{15}N value of the representative baseline, and TL_{base} is the trophic level of that baseline. Variation in $\delta^{15}N_{base}$ is common within systems; primary consumers are typically used due to longevity and reduced seasonality in δ^{15}N compared to primary producers (Cabana and Rasmussen 1994). In this work, the primary consumer *Paragrapsus gaimardii* (mottled shore crab) was considered to be the representative baseline in each region, and thus $TL_{base} = 2$.

Assessment of biomagnification was undertaken by calculation of trophic magnification factors (TMF):

$$\text{Log}_{10}\,(\text{THg/MeHg/Se}) = a + (b \times \delta^{15}N_{standard}) \quad (4)$$

where a is the point of intercept and b is the slope of the regression

$$TMF = 10^{b} \quad (5)$$

Trophic magnification is considered to occur when TMF > 1 (i.e., slope $b > 0.1$). Biomagnification regression models were run on the full data set by region and then on a refined data set resulting from the BSIMM. The expectation is that the BSIMM data set will increase regression fit by including only prey species with a mean proportional contribution to flathead diet of > 5% within that region. Variation in model fit between the full data set and the SIAR regressions was assessed by comparison of R^2 values, and variation in biomagnification was assessed by comparison of TMF. Variation in biomagnification between regions within the BSIMM food web was assessed by ANCOVA, with prior testing of normality using the Shapiro–Wilk test. Variations in % MeHg and Se : Hg with δ^{15}N and between regions was also tested using linear regressions and ANCOVA.

Results

Stable isotopes—Although the species consumed by sand flathead varied between regions, crustaceans made up the majority of the prey species throughout all regions in this study (Table 1). Within both Derwent Estuary regions (RB and ME), the benthic crab *P. gaimardii* contributed the highest biomass ($\%W$), while in the reference region, the squat lobster *Munida haswelli* was the preferred prey (Table 1). Fish species contributed between 1.2% and 20%W of the prey found in the gut contents (Table 1).

The δ^{13}C values ranged between −22.8‰ and −14.5‰ (Fig. 2). It was possible to differentiate the benthic and pelagic species in all three regions on the basis of the δ^{13}C values, with planktonic fractions being lighter in δ^{13}C (−19.7‰ to −22.8‰) than all other prey samples (−18.6‰ to −14.5‰). However, there was one notable exception to this, namely, the shrimp *Paleomon intermedius* from RB, which measured −20.7‰ (Fig. 2). There was no significant difference between the δ^{13}C values of sand flathead and the benthic prey species from RB (Kruskal–Wallis $p = 0.18$, degrees of freedom [df] = 43). However, δ^{13}C values in both ME and MB flathead were significantly higher than that of their benthic prey (Kruskal–Wallis $p < 0.01$, df = 40/16) but lower than the plankton (Fig. 2). Sand flathead from RB had higher δ^{13}C values than either of the other regions examined (Kruskal–Wallis $p < 0.01$, df = 15; Fig. 2).

The δ^{15}N values increased from prey species (8.5–13.6‰) to sand flathead (14.3–16.9‰), but only in the ME did plankton samples have lower δ^{15}N than other prey (Table 2). Mean fractionation of δ^{15}N between prey species and flathead increased from the RB region (4.5‰) through

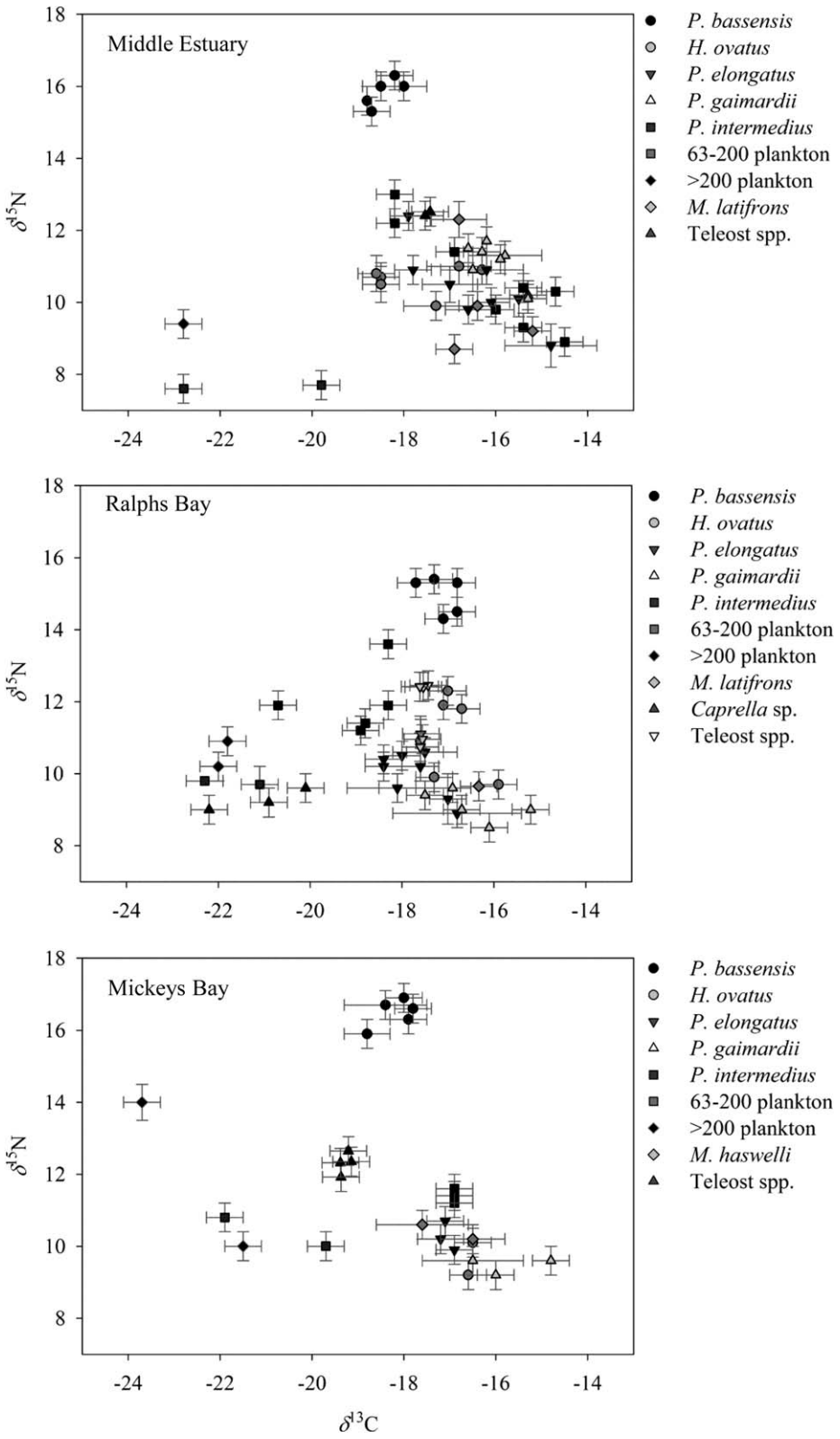

Fig. 2. δ^{13}C and δ^{15}N values for prey species of sand flathead (*Platycephalus bassensis*) from three locations in southern Tasmania. Points represent single samples with duplicate sample standard deviations. Derwent Estuary sample regions ME, RB, and the reference region MB. Species listed are *Platycephalus bassensis*, *Halicarcinus ovatus*, *Petrolisthes elongatus*, *Paragrapsus gaimardii*, *Palaemon intermedius*, *Macrophthalmus latifrons*, *Munida haswelli*, *Caprella* sp., Teleost spp. 63–200 = 63–200 μm plankton fraction; > 200 = > 200 μm plankton fraction.

Table 2. TL and mean concentrations (dry weight) of THg, MeHg, Se, %MeHg, and Se : Hg ratio with standard deviation from two Derwent Estuary regions (ME andRB) and a reference region (MB) for selected species in the sand flathead (*Platycephalus bassensis*) food web. TL is calculated from $TL = [(\delta^{15}N_{species} - \delta^{15}N_{base})/\Delta\ \delta^{15}N] + TL_{base}$, where $\delta^{15}N_{species}$ is the $\delta^{15}N$ value of the species in question, $\delta^{15}N_{base}$ is the $\delta^{15}N$ value of representative baseline (*P. gaimardii*) and TL_{base} is the trophic level of that baseline. Lowercase letters (a, b, c) denote significant differences ($p = 0.05$) between regions.

	n			TL			THg			MeHg			%MeHg			Se			Se : Hg		
Species	ME	RB	MB	ME	RB	MB	ME	RB	MB	ME	RB	MB	ME	RB	MB	ME	RB	MB	ME	RB	MB
63–200 μm plankton	4	2	2	1.01	2.23	2.28	0.08 (0.05)	0.3 (0.14)	0.1 (0.05)	0.02	0.02 (0.02)	0.00	—	11.37 (10.28)	9.51	0.94 (0.73)	1.93 (0.28)	1.71	6.29	18.35 (3.61)	60.05 (26.64)
>200 μm plankton	6	4	5	1.52	2.47	2.74	0.13 (0.08)	0.11 (0.05)	0.09 (0.05)	0.02 (0.01)	—	0.01 (0.00)	3.81 (0.95)	—	7.08	1.53 (0.63)	0.60	0.55	14.7 (6.01)	24.38 (7.29)	65.59 (26.95)
Paragrapsus gaimardii Mottled shore crab	40	21	9	2.00	2.00	2.00	0.64a (0.46)	0.66a (0.78)	0.19b (0.24)	0.11a (0.08)	0.19a (0.26)	0.03b (0.00)	24.97 (20.72)	46.36 (26.67)	26.32 (16.57)	1.12 (0.49)	1.12 (0.32)	1.52 (0.87)	7.87b (9.74)	32.01a (55.2)	33.82a (25.47)
Petrolisthes elongates New Zealand half-crab	13	12	10	1.82	2.34	2.24	0.09a (0.06)	0.09a (0.04)	0.03b (0.02)	0.04 (0.03)	0.08 (0.04)	0.06 (0.01)	46.10 (60.88)	45.06 (35.22)	100.0	1.57 (0.15)	1.36 (0.06)	1.18 (0.14)	42.36b (9.41)	42.03b (6.07)	101.01a (1.56)
Halicarcinus ovatus Spider crab	3	6	4	1.93	2.63	2.06	0.57 (0.25)	0.72 (0.18)	0.07 (0.00)	0.12 (0.06)	0.21 (0.04)	0.05 (0.00)	14.92 (2.34)	29.24 (1.23)	71.43 (5.45)	3.74 (0.10)	0.57 (0.01)	—	8.23 (0.20)	2.89 (0.50)	5.45
Palaemon intermedius Caridean shrimp	12	6	4	1.89	2.90	2.57	0.34 (0.17)	0.21 (0.16)	0.01 (0.05)	0.11 (0.03)	0.29 (0.13)	0.05 (0.00)	36.89 (25.06)	62.07 (26.29)	100.0	1.95 (0.22)	1.82 (0.33)	2.62 (0.82)	18.47 (14.84)	12.11 (4.94)	71.76
Munida haswelli squat lobster	—	—	3	—	—	2.28	—	—	0.03 (0.00)	—	—	0.04 (0.00)	—	—	100.0	—	—	1.58 (0.31)	—	—	104.2
Macrophthalmus latifrons Southern Sentinel Crab	9	—	—	1.7	2.21	—	0.59 (0.27)	—	—	0.17 (0.13)	—	—	26.33 (19.84)	—	—	1.37 (0.27)	—	—	6.40 (1.62)	—	—
Teleost spp. Prey fish	2	4	3	2.42	2.73	2.84	0.35 (0.02)	0.34 (0.06)	0.19 (0.02)	0.30 (0.02)	0.31 (0.09)	0.19 (0.06)	85.86 (11.42)	92.76 (21.71)	100.13 (33.24)	1.56 (0.18)	1.51 (0.28)	1.62 (0.28)	11.51 (2.01)	11.74 (3.58)	22.20 (5.42)
Platycephalus bassensis Sand flathead	20	20	20	3.45	3.77	4.06	1.28a (0.71)	1.34a (0.61)	0.32b (0.16)	1.31a (0.68)	1.40a (2.16)	0.30b (0.51)	103.31 (29.96)	106.12 (25.58)	91.42 (20.63)	1.22 (0.22)	1.29 (0.33)	1.30 (0.82)	9.43b (13.81)	3.31c (1.37)	12.07a (5.55)

ME (5.4‰) to MB (5.6‰), while trophic level (TL) calculations revealed that TL was highest in sand flathead from the reference region (TL = 4.06) and lowest in the ME (TL = 3.45; Table 2). Plankton TL ranged from 1.01 to 2.74, indicating highly variable $\delta^{15}N$ values. Benthic prey species TL varied between 1.70 and 2.84 across the regions, suggesting that they were largely primary consumers (Table 2).

The BSIMM estimated that the largest proportional contribution to diet within both Derwent Estuary regions was from *P. gaimardii* (Fig. 3). *Macrophthalmus latifrons* and *Petrolithes elongatus* contributed > 5% to the mean proportion of flathead diet in both the ME and RB regions, while in RB prey fish species also contributed > 5% (Fig. 3). In the reference region (MB) there was a large dietary shift, with teleost prey species being the principal proportional source to diet, with other significant contributions from *M. haswelli, P. gaimardii*, *Halicarcinus ovatus*, and *Palaemon intermedius* (Fig. 3). In all three regions plankton contributed < 5% to diet (Fig. 3).

Trace element concentrations—A summary of concentrations measured in each species is provided in Table 2. Note that low replication levels and the absence of some species from the flathead diet in certain regions prevented statistical comparison of those species. THg ($F_{2,59} = 4.84$, $p = 0.01$) and MeHg ($F_{2,51} = 4.61$, $p = 0.01$) concentrations differed significantly between the Derwent Estuary and the reference region (MB) in the principal prey species *P. gaimardii*, but there was no difference in these concentrations between the regions within the Derwent Estuary (Table 2). Similarly, THg concentrations in *P. elongatus* did not differ between RB and ME, but concentrations were lower in MB than in the Derwent Estuary ($F_{2,20} = 19.21$, $p < 0.001$). Sand flathead THg ($F_{2,59} = 14.54$, $p = 0.01$) and MeHg $F_{2,59} = 9.84$, $p = 0.01$) concentrations were significantly higher in the Derwent Estuary (RB and ME) than in MB. However, neither Se concentration nor %MeHg differed between regions in any species examined (Table 2). Molar ratios of Se : Hg varied between species and regions with the reference region having larger Se molar advantage over the Derwent Estuary regions in all but one species (*H. ovatus*; Table 2).

Biomagnification—Biomagnification of THg, MeHg, and Se was assessed by regressing $\log_{10}$ contaminant concentration against $\delta^{15}N_{standard}$ within region. THg and MeHg increased with $\delta^{15}N_{std}$, with the regression strength increasing significantly with MeHg in all regions (Fig. 4). The regression fit of $\delta^{15}N_{std}$–THg, and $\delta^{15}N_{std}$–MeHg (Fig. 4), improved significantly in the RB and MB regions within BSIMM-refined trophic models compared to non-BSIMM models. RB THg regression fit increased by 11%, while MB increased by 31%. For MeHg, BSIMM increased model fit in RB by 10% and MB by 6%. No improvement in regression fit was evident in ME between BSIMM trophic models and non-BSIMM models for either $\delta^{15}N_{std}$–THg (Fig. 4) or $\delta^{15}N_{std}$–MeHg (Fig. 4). Within the BSIMM-refined food web, there was no difference in regression slopes (biomagnification) between regions for

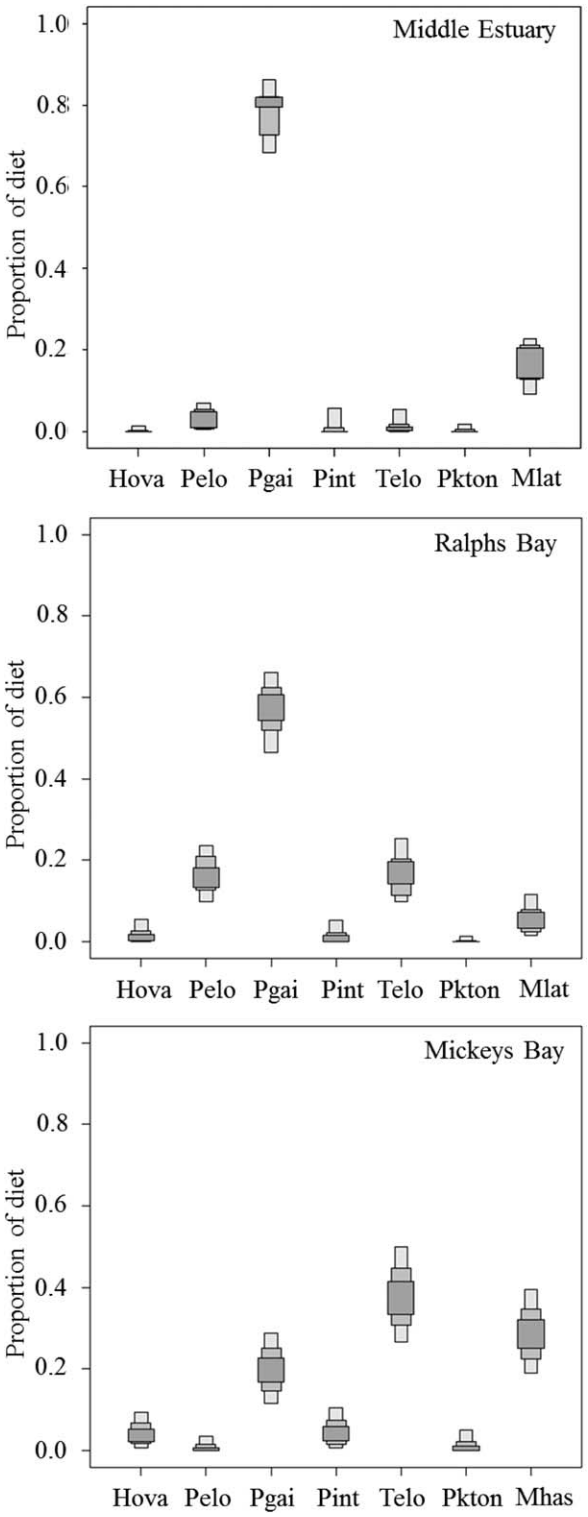

Fig. 3. Bayesian isotope mixing model contributions to diet of sand flathead from three regions in southern Tasmania (ME, RB, and MB). The SIAR model predictions of proportional contribution to diet with 95%, 75%, and 25% credibility intervals. Prey sources modeled are *Halicarcinus ovatus* (Hova), *Petrolisthes elongatus* (Pelo), *Paragrapsus gaimardii* (Pgai), *Palaemon intermedius* (Pint), 63–200 μm plankton (63–200), > 200 μm plankton (> 200), *Macrophthalmus latifrons* (Mlat), and *Munida haswelli* (Mhas).

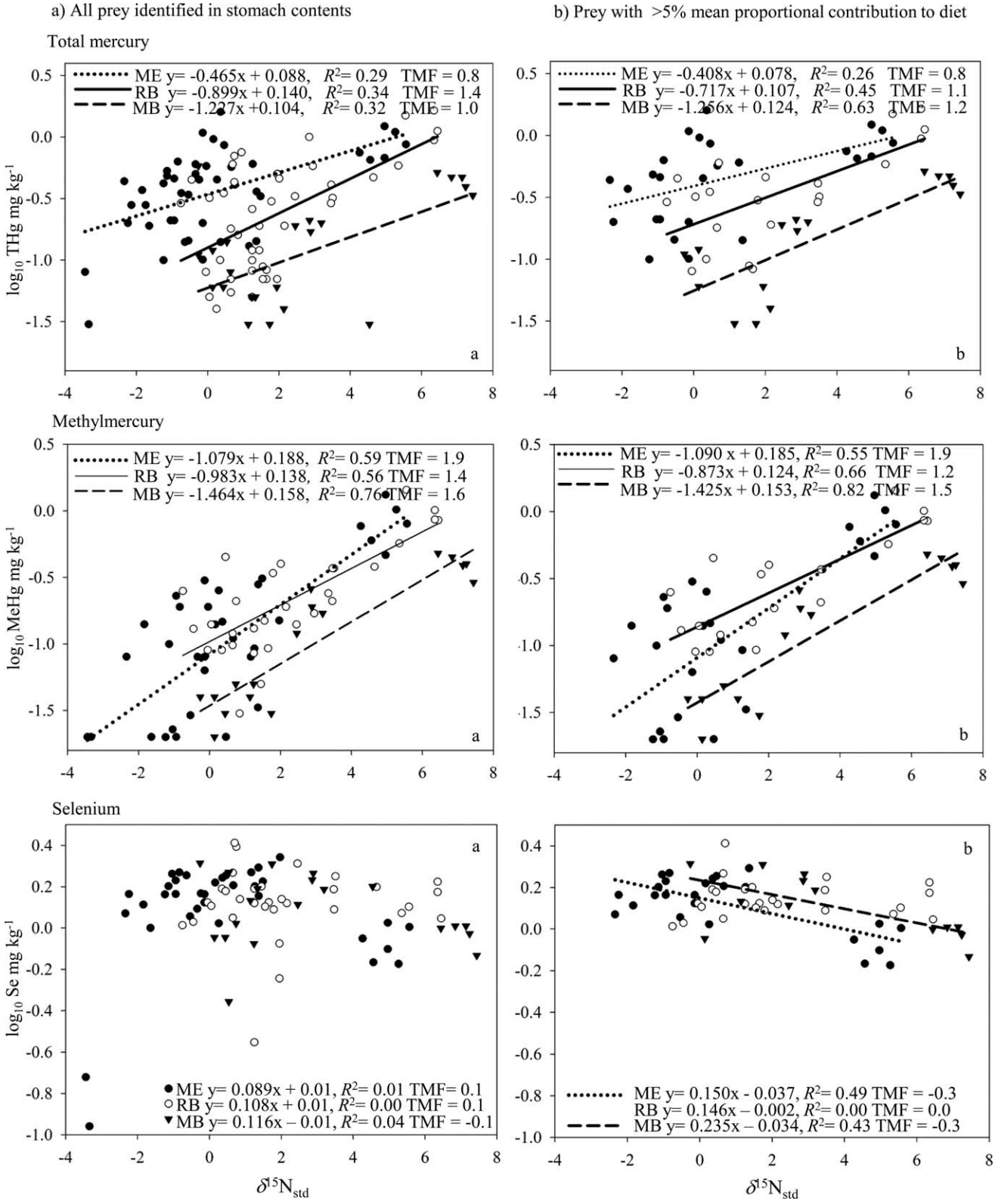

Fig. 4. Linear regressions (R^2) between $\delta^{15}N_{std}$ and $\log_{10}$ concentrations of THg, MeHg, and Se in sand flathead food webs from two Derwent Estuary regions (ME and RB) and the reference region (MB). (a) Regressions including all prey species identified in sand flathead gut contents and (b) regressions of prey found to account for $> 5\%$ mean proportional contribution to sand flathead diet based on SIAR mixing model.

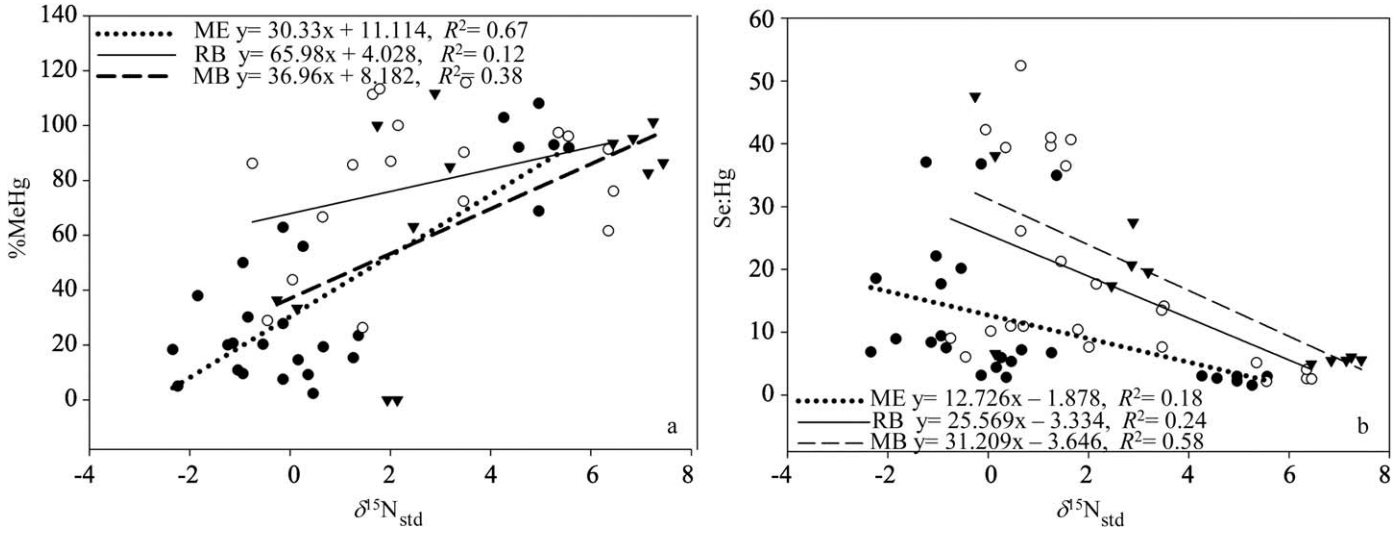

Fig. 5. Linear regression coefficients (R^2) of select species identified by SIAR mixing model in sand flathead food webs from two Derwent Estuary regions (ME and RB) and the reference region, MB. Graphs presented are $\delta^{15}N_{std}$ vs. % MeHg and $\delta^{15}N_{std}$ vs. Se : Hg molar ratios.

either THg ($F_{2,60} = 1.21$, $p = 0.30$) or MeHg ($F_{2,58} = 1.27$, $p = 0.29$), but the point of intercept varied significantly between regions for THg ($F_{2,60} = 14.84$, $p < 0.001$) and MeHg ($F_{2,58} = 9.72$, $p < 0.001$; Fig. 4). Se showed no correlation with $\delta^{15}N_{std}$ in any region (Fig. 4), but within the BSIMM food web Se showed a weak but significant decline in ME and MB (Fig. 4), although there was no difference in point of intercept between regions ($F_{2,60} = 1.21$, $p = 0.30$).

TMF_{MeHg} and TMF_{THg} (except at ME; Fig. 4), were ≥ 1, suggesting biomagnification of both Hg forms between trophic levels (Fig. 4). TMF_{MeHg} was higher than TMF_{THg} in all regions (Fig. 4). However, regional differences in TMF_{THg} were reduced for BSIMM regressions compared to the regional variability in the full data set (Fig. 4). TMF_{MeHg} did not alter between BSIMM regressions and the full data set but declined between regions with ME > MB > RB (Fig. 4). TMF_{Se} did not exceed 1 at any location, suggesting that Se biomagnification was not occurring in any region (Fig. 4).

In all regions, %MeHg within BSIMM-refined food webs increased at a similar rate to $\delta^{15}N_{std}$ ($F_{2,55} = 2.57$, $p = 0.09$), although the regression strength varied (Fig. 5). All regions exhibited equal negative regressions between Se : Hg and $\delta^{15}N_{std}$ ($F_{2,59} = 0.88$, $p = 0.42$), with a similar point of intercept ($F_{2,59} = 2.54$, $p = 0.09$; Fig. 5).

Discussion

This study is the first to use BSIMM to inform Hg trophic magnification regressions. We found that BSIMM-adjusted regressions provided better model fit between Hg (THg and MeHg) concentrations and trophic level ($\delta^{15}N$) than nonadjusted regressions. The BSIMM trophic models removed inconsequential planktonic and benthic prey species, reducing variability in contaminant concentrations and uncertainty in prey trophic level. This significantly altered points of intercept and produced less variable models of trophic magnification to sand flathead than using the full data set. The BSIMM model defined the trophic pathway between sand flathead and benthic prey, suggesting specific benthic dietary sources of contaminants that varied between regions in this study. The BSIMM model enabled discrimination between prey species with similar isotopic values, and this would not have been possible with other isotope models where dietary inputs are not included (Bond and Diamond 2011). This study suggests that, by removing bias associated with nonsignificant prey Hg concentrations, BSIMM provides an approach that significantly reduces uncertainty in Hg biomagnification studies where an understanding of Hg pathways to predators is required. This technique will be particularly beneficial for monitoring and toxicity risk assessments for predatory species, particularly those of high conservation value and those that are eaten by humans.

The capacity of the BSIMM model to predict dietary contribution is dependent on assumptions regarding the trophic enrichment factors (TEF) in $\delta^{15}N$ and $\delta^{13}C$ between predator and prey (Bond and Diamond 2011). Unfortunately, in this study, TEF were not available for individual predators or prey, and therefore global means were used (Post 2002). Although the BSIMM model is slightly weakened by the reliance on global mean data, the incorporation of the dietary information into the model strengthened the output and separated the contributions of the various prey to the diet (Bond and Diamond 2011). Future experiments to verify TEF for the species in this study could be used to reduce uncertainty in the BSIMM model and thereby improve the accuracy of the trophic regressions.

Both THg and MeHg showed significant biomagnification in all regions, with MeHg exhibiting higher biomagnification throughout. BSIMM-informed TMF_{THg} and TMF_{MeHg} were spatially variable, suggesting a difference in biomagnification rates between regions. However, the similarity between the regional regression slopes suggests that any difference is likely to be nonsignificant. The TMF_{THg} and TMF_{MeHg} across the regions were similar to TMF

reported in other work (Chen et al. 2008), supporting the concept that there is considerable stability in THg and MeHg TMF across latitudes and aquatic systems (Campbell et al. 2005; Coelho et al. 2013). This is despite significant differences in Hg contamination sources between systems (Chen et al. 2008). Elevated MeHg regressions and the increase of %MeHg between the successive trophic levels in this study suggest that MeHg is being preferentially biomagnified between trophic levels (Chen et al. 2008). The lower regression strength observed in THg–$\delta^{15}N_{std}$ regressions against MeHg–$\delta^{15}N_{std}$ would appear to be the product of a number of factors. These include (1) selective uptake of MeHg over inorganic Hg within the guts of predators as a result of cellular partitioning (Mason et al. 1995), (2) bioaccumulation of inorganic species of Hg through dissolved or sedimentary phases (Borgå et al. 2012; Coelho et al. 2013), (3) the fraction of THg as MeHg in invertebrates varying widely as a result of feeding strategies and species-specific habits (Evers et al. 2008; Coelho et al. 2013), and (4) the insolubility of inorganic Hg, such as mercury selenide (HgSe), contained within prey, making it unavailable for dietary absorption (Ralston and Raymond 2010). All of these conditions would reduce regression strength.

The BSIMM model refined the pathway between sand flathead and benthic prey, suggesting that the primary source of contaminants was benthic, consistent with previous studies that have linked Hg biotransfer between sediments and benthic predatory fish species (Chen et al. 2008; Gehrke et al. 2011). The significant variation in point of intercept between regions for MeHg, THg, and %MeHg suggests a differential bioavailability in Hg forms at the base of sand flathead food webs. The ME region of the Derwent Estuary has significantly higher sediment THg concentrations than RB (Jones et al. 2003, 2014), consistent with the higher point of intercept for THg and suggesting an increased uptake of THg at the food web base. In contrast, the higher intercept of MeHg in RB compared to ME and MB suggests that the bioavailability of MeHg in this region may be higher. The concept of RB as a potential methylation hot spot has been suggested before (Jones et al. 2013*b*) and would seem to imply that significant portions of that THg load in ME are biologically unavailable.

Previous work has found evidence of increased Se concentration with higher trophic levels (Barwick and Maher 2003; Kehrig et al. 2009), but this was not observed in the present study, as no evidence of biomagnification was present (Campbell et al. 2005). Se as a micronutrient is taken up, stored, and distributed as required by organisms (Yang et al. 2008). It is known to reduce Hg toxicity when at molar advantage (Peterson et al. 2009). Se maintained a molar excess over Hg in all species examined in this study, with Se concentrations never reaching those considered to be a toxic threat (Lemly 1996). Exceptionally large Se molar advantages have been recorded through lower trophic groups (Chen et al. 2001; Belzile et al. 2006, Karimi et al. 2013), but these molar advantages tend to decrease up the food chain to higher organisms (Yang et al. 2008; Kehrig et al. 2009; Fang et al. 2011). This relationship was also evident in the present study, with the reduced molar advantage with increasing trophic level being the result of the biomagnification of Hg across trophic levels, as Se concentrations showed either no biomagnification or weak reductions with increasing $\delta^{15}N$. The stability of the Se concentrations across the food web may be the result of a metabolic balancing act in which Se molar advantage over Hg is offset against maintaining Se concentrations at a level that does not cause toxicity problems (Lemly 1996). Overall, the results of this study indicate that there is no evidence for Se biomagnification or any toxic threat to organisms in the Derwent Estuary and that there is a sufficient concentration of Se in the system to maintain basal metabolic reactions over biomagnified Hg species throughout the sand flathead food web.

Trophic models of food pathways, based on $\delta^{15}N$, have been shown to predict changes in Hg concentrations in fish (Tom et al. 2010). The results of this study show that BSIMM can be applied prior to the running of the trophic models to refine dietary contributions and further reduce uncertainty in Hg transfer routes. The BSIMM conducted in this work should be considered as a useful additional tool for future assessments of Hg biomagnification when there is a need to define food pathways to top predators and for species eaten by humans. The results clearly suggest that, despite the presence of significant Hg pollution within the Derwent (Jones et al. 2003) and elevated Hg concentrations in biota, the rate at which Hg is biomagnified between trophic levels is not significantly elevated against other global regions with no direct Hg input (Campbell et al. 2005; Chen et al. 2008). This work also reestablishes the theory that, provided that trophic status is similar throughout a food web, it is the bioavailability of Hg at the base of the food web that is the key determinant of Hg concentration in benthic estuarine predators.

Acknowledgments

We acknowledge Nyrstar, Hobart, for continued support of this project, in particular Todd Milne and James Burke. We also thank Jason Whitehead and Christine Coughanowr at the Derwent Estuary Program for in-kind support and Warren Corns and Bin Chen of Peter Stockwell Analytical (PSA, UK) for providing access to specialist analytical instruments and expertise for determining the trace element loadings presented in this article. We thank Sean Tracey for proofreading this manuscript and Thomas Rodemann of the Central Science Laboratory, University of Tasmania, for the elemental analysis. We also thank the reviewers of this manuscript whose input greatly improved this article. This work was supported by the Australian Nuclear Science and Technology Organisation under Australian Institute of Nuclear Science and Engineering grants (ALNGRA10090 and ALNGRA11069) and a Seafood Cooperative Research Centre Research grant for the trace element analysis and additional experimental costs.

References

Adams, D. H., and R. Paperno. 2012. Stable isotopes and mercury in a model estuarine fish: Multibasin comparisons with water quality, community structure, and available prey base. Sci. Total Environ. **414:** 445–455, doi:10.1016/j.scitotenv.2011.10.014

Al-Reasi, H. A., F. A. Ababneh, and D. R. Lean. 2007. Evaluating mercury biomagnification in fish from a tropical marine environment using stable isotopes ($\delta^{13}C$ and $\delta^{15}N$). Environ. Toxicol. Chem. **26:** 1572–1581, doi:10.1897/06-359R.1

Barwick, M., and W. Maher. 2003. Biotransference and biomagnification of selenium copper, cadmium, zinc, arsenic and lead in a temperate seagrass ecosystem from Lake Macquarie Estuary, NSW, Australia. Mar. Environ. Res. **56:** 471–502, doi:10.1016/S0141-1136(03)00028-X

Belzile, N., Y. W. Chen, J. M. Gunn, J. Tong, Y. Alarie, T. Delonchamp, and C. Y. Lang. 2006. The effect of selenium on mercury assimilation by freshwater organisms. Can. J. Fish. Aquat. Sci. **63:** 1–10, doi:10.1139/f05-202

Beneditto, A., V. Bittar, P. Camargo, C. Rezende, and H. Kehrig. 2012. Mercury and nitrogen isotope in a marine species from a tropical coastal food web. Arch. Environ. Contam. Toxicol. **62:** 264–271, doi:10.1007/s00244-011-9701-z

Besser, J. M., T. J. Canfield, and T. W. La Point. 1993. Bioaccumulation of organic and inorganic selenium in a laboratory food chain. Environ. Toxicol. Chem. **12:** 57–72, doi:10.1002/etc.5620120108

Bloom, H., and G. Ayling. 1977. Heavy metals in the Derwent Estuary. Environ. Geol. **2:** 3–22, doi:10.1007/BF02430661

Bond, A. L., and A. W. Diamond. 2011. Recent Bayesian stable-isotope mixing models are highly sensitive to variation in discrimination factors. Ecol. Appl. **21:** 1017–1023, doi:10.1890/09-2409.1

Borgå, K., K. A. Kidd, D. C. G. Muir, O. Berglund, J. M. Conder, F. A. P. C. Gobas, J. Kucklick, O. Malm, and D. E. Powell. 2012. Trophic magnification factors: Considerations of ecology, ecosystems, and study design. Integr. Environ. Assess. Manag. **8:** 64–84, doi:10.1002/ieam.244

Cabana, G., and J. B. Rasmussen. 1994. Modelling food chain structure and contaminant bioaccumulation using stable nitrogen isotopes. Nature **372:** 255–257, doi:10.1038/372255a0

Campbell, L. M., R. J. Norstrom, K. A. Hobson, D. C. G. Muir, S. Backus, and A. T. Fisk. 2005. Mercury and other trace elements in a pelagic Arctic marine food web (Northwater Polynya, Baffin Bay). Sci. Total Environ. **351–352:** 247–263, doi:10.1016/j.scitotenv.2005.02.043

Chen, C., A. Amirbahman, N. Fisher, G. Harding, C. Lamborg, D. Nacci, and D. Taylor. 2008. Methylmercury in marine ecosystems: Spatial patterns and processes of production, bioaccumulation, and biomagnification. EcoHealth **5:** 399–408, doi:10.1007/s10393-008-0201-1

Chen, C. Y., M. Dionne, B. M. Mayes, D. M. Ward, S. Sturup, and B. P. Jackson. 2009. Mercury bioavailability and bioaccumulation in estuarine food webs in the Gulf of Maine. Environ. Sci. Technol. **43:** 1804–1810, doi:10.1021/es8017122

Chen, Y. W., Belzile, N., and Gunn, J. M. 2001. Antagonistic effect of selenium on mercury assimilation by fish populations near Sudbury metal smelters. Limnol. Oceanogr. **46:** 1814–1818, doi:10.4319/lo.2001.46.7.1814

Cheung, M. S., and W.-X. Wang. 2008. Analyzing biomagnification of metals in different marine food webs using nitrogen isotopes. Mar. Pollut. Bull. **56:** 2082–2088, doi:10.1016/j.marpolbul.2008.09.004

Coelho, J. P., C. L. Mieiro, A. C. Duarte, and M. A. Pardal. 2013. Mercury biomagnification in a contaminated estuary food web: Effects of age and trophic position using stable isotope analyses. Mar. Pollut. Bull. **69:** 110–115, doi:10.1016/j.marpolbul.2013.01.021

Cossa, D., M. Harmelin-Vivien, C. Mellon-Duval, V. Loizeau, B. Averty, S. Crochet, L. Chou, and J. F. Cadiou. 2012. Influences of bioavailability, trophic position, and growth on methylmercury in Hakes (*Merluccius merluccius*) from northwestern Mediterranean and Northeastern Atlantic. Environ. Sci. Technol. **46:** 4885–4893, doi:10.1021/es204269w

Dix, T. G., Martin, A., Ayling, G. M., Wilson, K. C., and D. A. Ratkowsky. 1975. Sand flathead (*Platycephalus bassensis*), an indicator species for mercury pollution in Tasmanian waters. Mar. Pollut. Bull. **6:** 142–144, doi:10.1016/0025-326X(75)90172-1

Evers, D., R. Mason, N. Kamman, C. Chen, A. Bogomolni, D. Taylor, C. Hammerschmidt, S. Jones, N. Burgess, K. Munney, and K. Parsons. 2008. Integrated mercury monitoring program for temperate estuarine and marine ecosystems on the North American Atlantic coast. EcoHealth **5:** 426–441, doi:10.1007/s10393-008-0205-x

Fang, G. C., D. H. Nam, and N. Basu. 2011. Mercury and selenium content of Taiwanese seafood. Food Addit. Contam. Part B **4:** 212–217.

France, R. L. 1995. Differentiation between littoral and pelagic food webs in lakes using stable carbon isotopes. Limnol. Oceanogr. **40:** 1310–1313, doi:10.4319/lo.1995.40.7.1310

Gehrke, G. E., J. D. Blum, D. G. Slotton, and B. K. Greenfield. 2011. Mercury isotopes link mercury in San Francisco Bay forage fish to surface sediments. Environ. Sci. Technol. **45:** 1264–1270, doi:10.1021/es103053y

Green, G., and C. Coughanowr, C. 2003. State of the Derwent Estuary 2003: a review of pollution sources, loads and environmental quality data from 1997–2003. Derwent Estuary Program - DPIWE, Hobart, Tasmania.

Hamilton, S. J. 2004. Review of selenium toxicity in the aquatic food chain. Sci. Total Environ. **326:** 1–31, doi:10.1016/j.scitotenv.2004.01.019

Hong, Y-S., P. Hull, E. Rifkin, and E. J. Bouwer. 2013. Bioaccumulation and biomagnification of mercury and selenium in the Sarasota Bay ecosystem. Environ. Toxicol. Chem. **32:** 1143–1152, doi:10.1002/etc.2169

Hyslop, E. J. 1980. Stomach contents analysis—a review of methods and their application. J. Fish Biol. **17:** 411–429, doi:10.1111/j.1095-8649.1980.tb02775.x

Jones, B. G., B. E. Chenhall, F. Debretsion, and A. C. Hutton. 2003. Geochemical comparisons between estuaries with non-industrialised and industrialised catchments: The Huon and Derwent River estuaries, Tasmania. Austral. J. Earth Sci. **50:** 653–667, doi:10.1111/j.1440-0952.2003.01018.x

Jones, H. J., E. C. V. Butler, and C. K. Macleod. 2013*a*. Spatial variability in selenium and mercury interactions in a key recreational fish species: Implications for human health and environmental monitoring. Mar. Pollut. Bull. **74:** 231–236, doi:10.1016/j.marpolbul.2013.06.052

———, K. M. Swadling, S. R. Tracey, and C. K. Macleod. 2013*b*. Long term trends of Hg uptake in resident fish from a polluted estuary. Mar. Pollut. Bull. **73:** 263–272, doi:10.1016/j.marpolbul.2013.04.032

———, ———, E. C. V. Butler, and C. K. Macleod. 2014. Complex patterns in fish–sediment mercury concentrations in a contaminated estuary: The influence of selenium co-contamination? Estuar. Coast. Shelf Sci. **37:** 14–22, doi:10.1016/j.ecss.2013.11.024

Karimi, R., M. G. Frisk, and N. S. Fisher. 2013. Contrasting food web factor and body size relationships with Hg and Se concentrations in marine biota. PLoS ONE **8:** e74695, doi:10.1371/journal.pone.0074695

Kehrig, H., T. Seixas, E. Palermo, A. Baêta, C. Castelo-Branco, O. Malm, and I. Moreira. 2009. The relationships between mercury and selenium in plankton and fish from a tropical food web. Environ. Sci. Pollut. Res. **16:** 10–24, doi:10.1007/s11356-008-0038-8

Lemly, A. D. 1996. Assessing the toxic threat of selenium to fish and aquatic birds. Environ. Monit. Assess. **43:** 19–35, doi:10.1007/BF00399568

Mason, R. P., J. R. Reinfelder, and F. M. M. Morel. 1995. Bioaccumulation of mercury and methylmercury. Water Air Soil Pollut. **80:** 915–921, doi:10.1007/BF01189744

Moore, J. W., and B. X. Semmens. 2008. Incorporating uncertainty and prior information into stable isotope mixing models. Ecology Letters **11:** 470–480, doi:10.1111/j.1461-0248.2008.01163.x

Parnell, A. C., R. Inger, S. Bearhop, and A. L. Jackson. 2010. Source partitioning using stable isotopes: Coping with too much variation. PLoS ONE **5:** e9672, doi:10.1371/journal.pone.0009672

Peterson, S. A., N. V. C. Ralston, P. D. Whanger, J. E. Oldfield, and W. D. Mosher. 2009. Selenium and mercury interactions with emphasis on fish tissue. Environ. Bioindicators **4:** 318–334, doi:10.1080/15555270903358428

Phillips, D. L., and J. W. Gregg. 2003. Source partitioning using stable isotopes: Coping with too many sources. Oecologia **136:** 261–269, doi:10.1007/s00442-003-1218-3

Post, D. M. 2002. Using stable isotopes to estimate trophic position: Models, methods, and assumptions. Ecology **83:** 703–718, doi:10.1890/0012-9658(2002)083[0703:USITET]2.0.CO;2

Ralston, N. V. C., and L. J. Raymond. 2010. Dietary selenium's protective effects against methylmercury toxicity. Toxicology **278:** 112–123, doi:10.1016/j.tox.2010.06.004

Tom, K. R., M. C. Newman, and J. Schmerfeld. 2010. Modeling mercury biomagnification (South River, Virginia, USA) to inform river management decision making. Environ. Toxicol. Chem. **29:** 1013–1020, doi:10.1002/etc.117

Verdouw, J., C. Macleod, B. Nowak, and J. Lyle. 2011. Implications of age, size and region on mercury contamination in estuarine fish species. Water Air Soil Pollut. **214:** 297–306, doi:10.1007/s11270-010-0424-y

Wang, W. X. 2002. Interactions of trace metals and different marine food chains. Mar. Ecol. Prog. Ser. **243:** 295–309, doi:10.3354/meps243295

Yang, D.-Y., Y.-W. Chen, J. M. Gunn, and N. Belzile. 2008. Selenium and mercury in organisms: Interactions and mechanisms. Environ. Rev. **16:** 71–92, doi:10.1139/A08-001

Associate editor: H. Maurice Valett

Received: 30 July 2013
Accepted: 05 February 2014
Amended: 24 February 2014